2

Katla and Eyjafjallajökull Volcanoes

Erik Sturkell[1,2,*], Páll Einarsson[3], Freysteinn Sigmundsson[2], Andy Hooper[4], Benedikt G. Ófeigsson[3], Halldór Geirsson[5] and Halldór Ólafsson[2]

[1]*Department of Earth Sciences, University of Gothenburg, Gothenburg, Sweden*
[2]*Nordic Volcanological Centre, University of Iceland, Askja, Sturlugata 7, IS-101 Reykjavík, Iceland*
[3]*Institute of Earth Sciences, University of Iceland, Askja, Sturlugata 7, IS-101 Reykjavík, Iceland*
[4]*Department of Earth Observation and Space Systems, Delft University of Technology, Delft, Netherlands*
[5]*Physics Department, Icelandic Meteorological Office, Reykjavík, Iceland*
*Correspondence and requests for materials should be addressed to Erik Sturkell (e-mail: erik.sturkell@guv.gu.se)

2.1. Introduction

The volcanic system of Katla is one of the most active ones in Iceland with at least twenty eruptions within the central volcano (Larsen, 2000) and one in its fissure swarm during the past 1,100 years. The volcano is covered mostly by the Mýrdalsjökull ice cap (Fig. 2.1); consequently, eruptions within the Katla central volcano are phreato-magmatic and capable of producing glacial bursts, that is, jökulhlaups. One of the most voluminous eruptions ($\sim 18.6\,km^3$, Thordarson and Larsen, 2007) in historical times since AD 874, the Eldgjá eruption AD 934–940, originated from the Katla fissure swarm extending from under the Mýrdalsjökull ice cap towards the north-east. Eruptions within the Katla caldera are much smaller with an upper limit of volume of approximately $2\,km^3$. The neighbouring volcano, 25 km to the west, is Eyjafjallajökull (also referred to as Eyjafjöll). It is currently much less active, with two eruptions during the past 1,100 years, occurring in tandem with Katla eruptions in 1612 and 1821–1823. The erupted volumes from the Eyjafjallajökull volcano have been negligible in historic times and range in the $0.1\,km^3$ scale. However, they can be extremely hazardous, as farms are located at the foot of the volcano, which rises 1.5 km from the agricultural plain.

As most eruptions are confined to the ice-covered Katla caldera area, huge amounts of meltwater are released in the beginning of an eruption. The path of these outburst floods depends critically on the location of the eruption site within the caldera, in relation to the present water divides under the ice within the caldera. In historical time, floods have on most occasions drained to the east and at a few instances also to the south. Jökulhlaups and fallout of tephra are primary hazards during a Katla eruption, and the proximity of the volcano to populated areas and to international flight paths makes it a potent threat.

Different chemistry and mineralogy distinguish the two volcanoes. FeTi basalt dominates volcanism of the Katla system. The Eyjafjallajökull volcanic system, on the contrary, has produced a suite of alkalic rocks ranging from ankaramites to hawaiite and minor silicic rocks (Jakobsson, 1979).

This compiled overview of geology, seismicity and crustal deformation is based principally on two research articles: Sturkell *et al.* (2003, 2008), the time series have been extended to include the collected data up to year 2008.

2.2. Tectonic Setting

The Katla and Eyjafjallajökull volcanoes are located outside the main zones of divergent plate motion. In south Iceland, the plate boundary is in a state of transition (e.g. Einarsson, 1991; Sigmundsson *et al.*, 1995; Sigmundsson, 2006). Plate divergence is presently taken up by two parallel rift zones: the Western Volcanic Zone (WVZ) and the Eastern Volcanic Zone (EVZ). Latitude-dependent variations in spreading rate are observed along both zones, with the EVZ accommodating 40–100% (Fig. 2.2) of the relative motion between the North American and Eurasian plates (LaFemina *et al.*, 2005). The spreading rate decreases southwards and active rifting terminates south of the Torfajökull volcano (Figs. 2.1 and 2.2), where the EVZ rift zone meets the transform boundary of the South Iceland Seismic Zone.

Large volcanoes characterize the segment of EVZ south of its intersection with the transform. Rifting structures on the surface are inconspicuous in this area. From the area between Torfajökull and Mýrdalsjökull to the Vestmannaeyjar islands, the influence of the EVZ is primarily seen in the decreasing alkalinity of rocks with increasing distance from the tip of the rift zone (Óskarsson *et al.*, 1982). The arguments are mainly geochemical and structural. FeTi volcanism, characteristic for propagating rifts, is found within this area, beginning 2–3 Myr ago (Jóhannesson *et al.*, 1990). Voluminous volcanism has created a plateau of FeTi basalt south of the Torfajökull area towards the south coast in Mýrdalur (Fig. 2.1). Therefore, Katla and the neighbouring volcanoes Eyjafjallajökull and Vestmannaeyjar (including
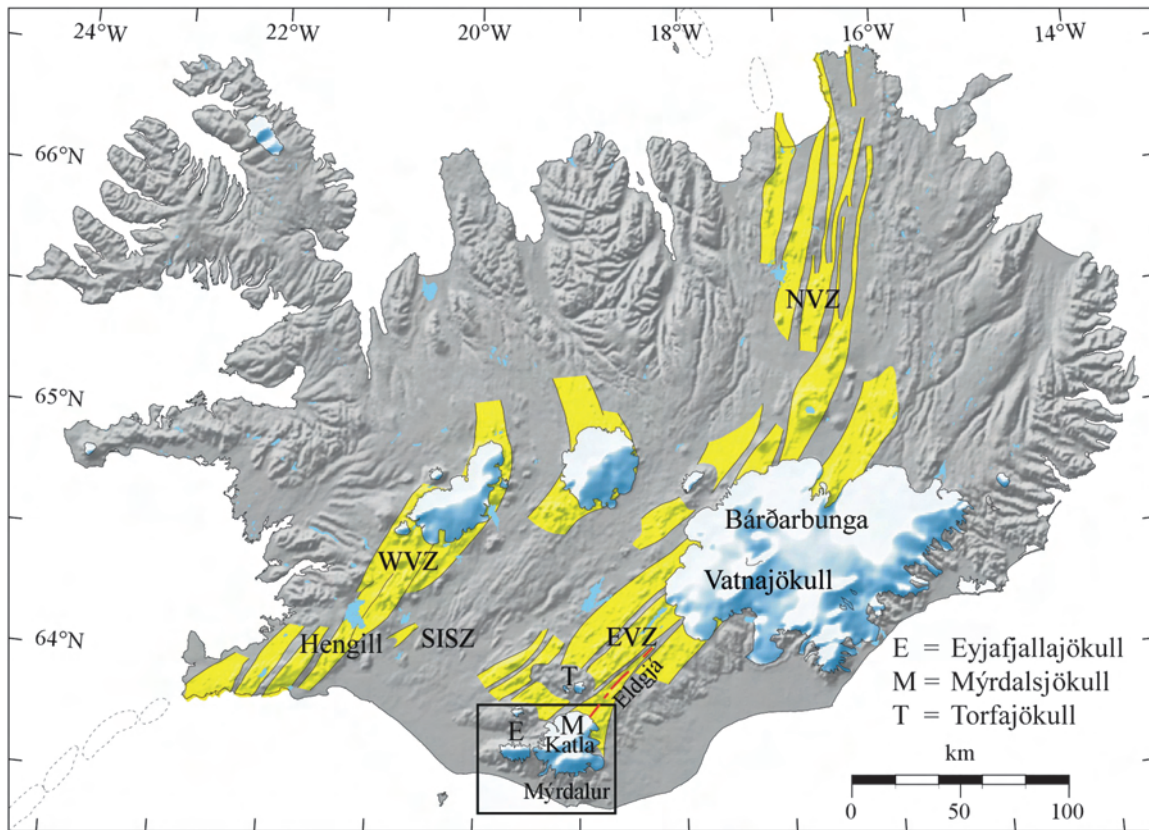
Fig. 2.1. Map of Iceland, showing the neo-volcanic zone consisting of individual volcanic systems coloured in yellow. Dashed lines mark submarine volcanic system and white areas are glaciers. The plate boundary in Iceland is expressed by different segments and is divided into the Northern Volcanic Zone (NVZ), the Western Volcanic Zone (WVZ), and the Eastern Volcanic Zone (EVZ) (Einarsson and Saemundsson, 1987). The EVZ and the WVZ are connected by the South Iceland Seismic Zone (SISZ). The area including Eyjafjallajökull and Katla is outlined with a box. The Eldgjá fissure is marked in red.

Fig. 2.2. Partition of plate spreading between the Western Volcanic Zone (WVZ) and the Eastern Volcanic Zone (EVZ). The spreading rate increases from north to south along the WVZ progressively from zero to 60% of spreading at the Hengill volcano and the opposite pattern is valid for the parallel EVZ. The surface structures associated with a rift in the EVZ terminates just north of the Mýrdalsjökull ice cap. The Hreppar micro-plate is located between the parallel spreading zones. Plate spreading data are taken from LaFemina et al. (2005).
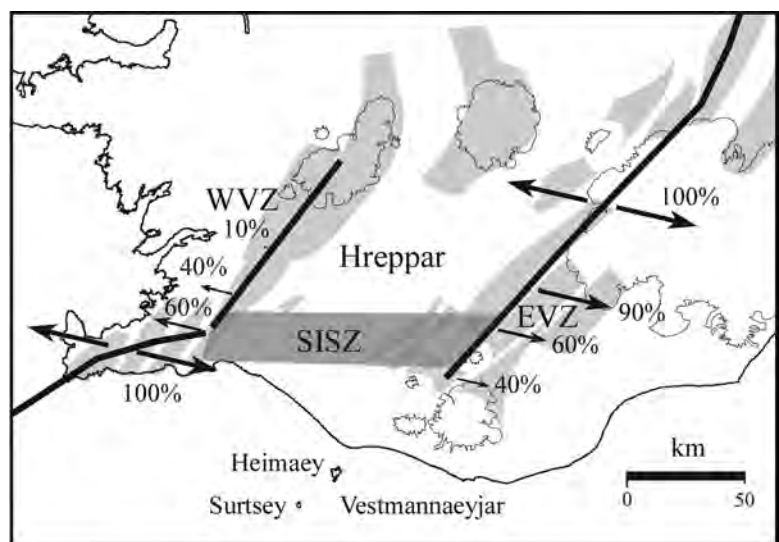
the Heimaey and Surtsey eruption sites, see Fig. 2.2) have spreading velocities consistent with a location on the stable Eurasian plate (LaFemina *et al.*, 2005; Geirsson *et al.*, 2006). Hence, Katla can be classified as an intraplate volcano, in spite of its occasional connection with rifting in the EVZ, exemplified by the AD 934 Eldgjá eruption (Fig. 2.1).

2.3. Structure and Eruptive Products of the Volcanoes

2.3.1. Katla

The Katla volcano hosts a 600- to 750-m-deep caldera filled with ice (Björnsson *et al.*, 2000). The caldera rim is
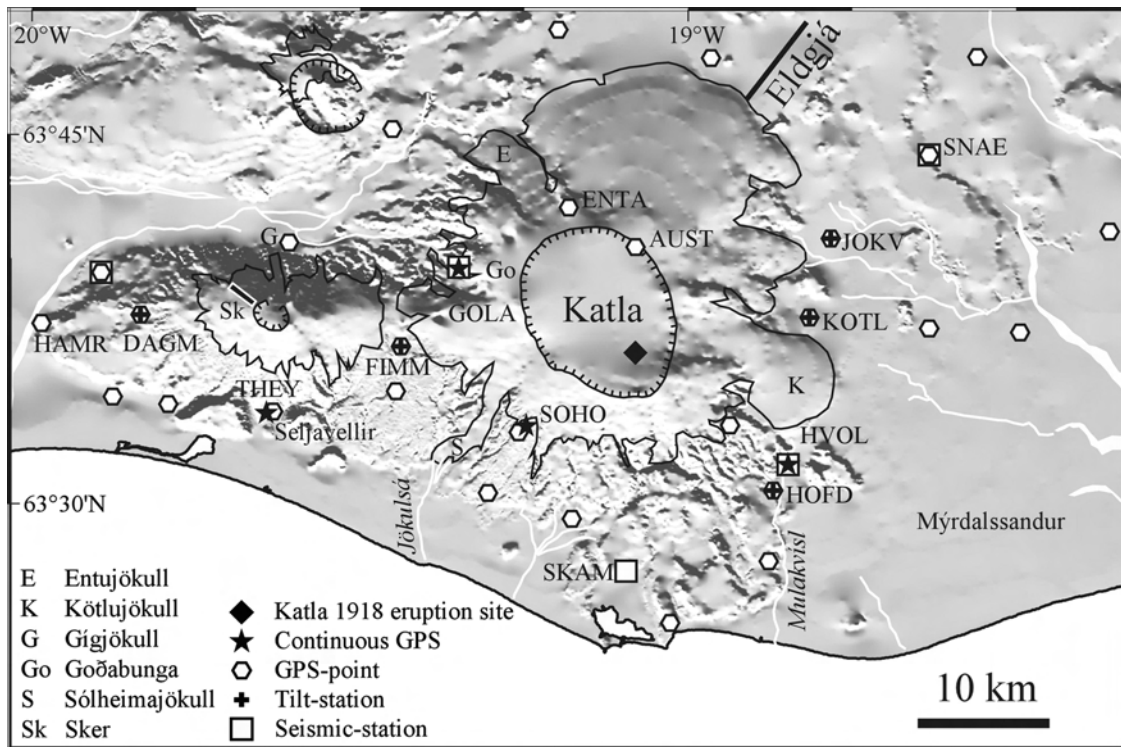
Fig. 2.3. The geodetic and seismic networks around Eyjafjallajökull and Katla (Mýrdalsjökull) showing campaign GPS, continuous GPS, tilt and seismic stations. On Mýrdalsjökull glacier, the hachured line is the Katla caldera, and the hachured line on Eyjafjallajökull marks the summit crater.

breached in three places, to the south-east, north-west and south-west. These gaps in the caldera rim provide outflow paths for ice in the caldera to feed the main outflow glaciers, Kötlujökull, Entujökull and Sólheimajökull (Fig. 2.3). Apart from the large Eldgjá flood lava eruption AD 934–940 (Thordarson *et al.*, 2001), all historical eruptions of the Katla volcanic system have occurred within the caldera (Larsen, 2000).

Volcanic products of Katla are primarily bimodal in composition, comprising alkali basalt and mildly alkalic rhyolites (Lacasse *et al.*, 2007). Intermediate rocks, mostly basalt-rhyolite hybrids and occasional hawaiite, are very subordinate (Lacasse *et al.*, 2007). Volumetrically, FeTi-rich basalt with aphyric appearance dominates. This is ascribed to rapid segregation of material from a large mantle source beneath a propagating rift (Sinton *et al.*, 1983). Silicic volcanism is an important component of Katla activity. At least twelve silicic tephra layers are known from Katla during the Holocene, between 1700 and 6600 BP (Larsen *et al.*, 1999; Larsen, 2000), and almost all known outcrops of Katla at the caldera rim and immediately outside of it are silicic (Jóhannesson *et al.*, 1990; Lacasse *et al.*, 2007). Katla tephras show that phreato-magmatic eruptions have taken place throughout the Holocene (Óladóttir *et al.*, 2005). The relatively homogeneous chemical composition of the products of large basaltic eruptions of Katla during the past 1,000 years seems to indicate that they have not had time to evolve in a shallow magma chamber (Óladóttir *et al.*, 2005, 2008). The wide range of composition for Katla magmas in general (Lacasse *et al.*, 2007), however,

points to a complicated magma plumbing system, which may even change significantly on a time scale of thousands of years (Óladóttir *et al.*, 2008).

Seismic undershooting within the Katla caldera has revealed a zone where P-wave velocities are reduced and S-waves are absent; this anomaly is interpreted as evidence of a magma chamber (Guðmundsson *et al.*, 1994). Moreover, results from an aeromagnetic survey indicate the presence of a non-magnetic body within the region of the postulated magma chamber (Jónsson and Kristjánsson, 2000).

2.3.2. Eyjafjallajökull

The Eyjafjallajökull volcano is an elongated, flat cone of about 1,600 m height. The Eyjafjallajökull glacier, up to 200 m thick (Guðmundsson and Högnadóttir, 2005), covers the volcano and its elliptical 2.5-km-wide summit crater (Fig. 2.3). The outlet glacier Gígjökull originates from the crater and flows towards the north through an opening in the crater rim. The most recent eruption in 1821–1823 occurred within the crater close to its southern rim and produced intermediate to acid tephra (Thoroddsen, 1925).

The Eyjafjallajökull volcano has an alkaline composition, similar to other off-rift volcanoes in Iceland. This type of volcano generates relatively small amounts of material; typically 0.1 km^3, during each eruption. Most eruptive fissures and crater rows at Eyjafjallajökull are E-W orientated, but occasional radial fissures are

observed around the summit of the volcano. The most conspicuous radial eruptive fissure is Sker (Fig. 2.3). In the area SSE of the summit crater and NE of the Seljavellir farm (Fig. 2.3), Jónsson (1998) reports the presence of highly altered rocks that are cut by numerous dikes and veins. This area is interpreted to be the oldest part of the Eyjafjallajökull volcano, with a suggested age of more than 0.78 Myr. If this age estimate is accurate, Eyjafjallajökull is one of the oldest active volcanoes in Iceland. The most pronounced expression of geothermal activity at Eyjafjallajökull is confined to its south flank, in the area around Seljavellir (Fig. 2.3). This area of geothermal activity correlates with the location of recently formed intrusions.

2.4. Recent Unrest in Katla

2.4.1. The 1918 Eruption

The latest large eruption of Katla began on 12 October 1918, lasting for some three weeks (Jóhannsson, 1919; Sveinsson, 1919). It was basaltic in composition, and the eruption site was near the southeast rim of the Katla caldera, beneath about 400 m of ice. A debris-laden jökulhlaup was seen propagating over Mýrdalssandur sand plains (Fig. 2.3) a few hours from the onset of the eruption. The 1918 eruption of Katla was large, but estimates of the total volume of erupted material vary. The amount of tephra fallout is estimated to be 0.7 km^3 (Eggertsson, 1919), and the volume of water-transported material is estimated at between 0.7 and 1.6 km^3 (Larsen, 2000). The dense-rock equivalent may have been as high as 1 km^3.

2.4.2. The 1955 Event

It is possible that a short-lived subglacial eruption took place in 1955 on the eastern rim of the Katla caldera; however, no tephra erupted into the atmosphere. Instead, two shallow ice cauldrons formed on the surface of Mýrdalsjökull and a small jökulhlaup drained from Kötlujökull glacier tongue (Rist, 1967; Thórarinsson, 1975).

2.4.3. The 1999–2005 Episode

In July 1999, an unexpected jökulhlaup drained from Mýrdalsjökull. Its timing is marked in Fig. 2.4 and is followed by elevated earthquake activity. This short-lived jökulhlaup was preceded several hours earlier by earthquakes and pulses of low-frequency tremor that originated from Mýrdalsjökull. Inspection of Mýrdalsjökull revealed a newly formed surface depression (ice cauldron) near to the epicentres of the earthquake swarm that preceded the jökulhlaup. The latest Katla eruption to break the ice surface took place in 1918. During the weeks following the 1999 jökulhlaup, increased geothermal activity was detected along the caldera rim, as manifest by the deepening of pre-existing ice cauldrons (Guðmundsson *et al.*, 2007).

From 2000 until 2004, uplift at the Global Positioning System (GPS) point AUST occurred at a rate of 1.7 cm/yr (Figs. 2.3 and 2.5), but interferometric measurements of deformation from radar satellites (InSAR) indicate no simultaneous uplift of the volcano flanks. Figure 2.6A shows the derived displacement vectors from benchmarks on and around Mýrdalsjökull, relative to stable Eurasia. Vertical uplift and radial displacement from the caldera centre were observed.

Using a point source model, these data place the centre of the magma chamber at 4.9 km depth beneath the northern part of the caldera. However, this depth may be overestimated because of a progressive decrease in the mass of the overlying ice cap, in reality, the depth may be only 2–3 km. About 0.01 km^3 of magma has accumulated between 1999 and 2005. This value is considerably less than the estimated 1 km^3 of material erupted during the latest eruption of Katla in 1918.

2.5. Recent Unrest in Eyjafjallajökull

Since 1994, the ice-capped Eyjafjallajökull volcano, situated 25 km west of Katla, has generated by far the largest amount of crustal deformation (Sturkell *et al.*, 2003). In 1994, and again in 1999, magma intrusion was detected under the southern slopes of Eyjafjallajökull. These intrusions had their centre of uplift approximately 4 km southeast of the summit crater of the volcano (Sturkell *et al.*, 2003; Pedersen and Sigmundsson, 2004, 2006) and were associated with considerable seismic activity (e.g. Dahm and Brandsdóttir, 1997). After the intrusion event in 1999, crustal deformation and earthquake activity at Eyjafjallajökull (Fig. 2.4) have remained low (Sturkell *et al.*, 2006).

This is, however, not the only known case of simultaneous unrest of Eyjafjallajökull and Katla. The two volcanoes apparently erupted in 1612, and the Eyjafjallajökull eruption of 1821–1823 was immediately followed by an eruption of Katla (Thoroddsen, 1925). These are the only known eruptions of Eyjafjallajökull in historic times.

2.6. Earthquakes

2.6.1. Seismic Activity of the Katla and Eyjafjallajökull Region

Katla stands out among Icelandic volcanoes for its high and persistent seismic activity. The only other volcanoes that compare to Katla in this respect are Hengill and Bárðarbunga (Fig. 2.1) (Einarsson, 1991; Jakobsdóttir, 2008), both of which are located on main branches of the plate boundary. As Katla is located at some distance from the main deformation zone of the plate boundary, its high seismicity is somewhat unique.

The seismicity of the Mýrdalsjökull region forms three distinct groups (Figs. 2.4 and 2.7), within the Katla caldera, at Goðabunga on the western flank of Katla and beneath Eyjafjallajökull. Seismic characteristics of
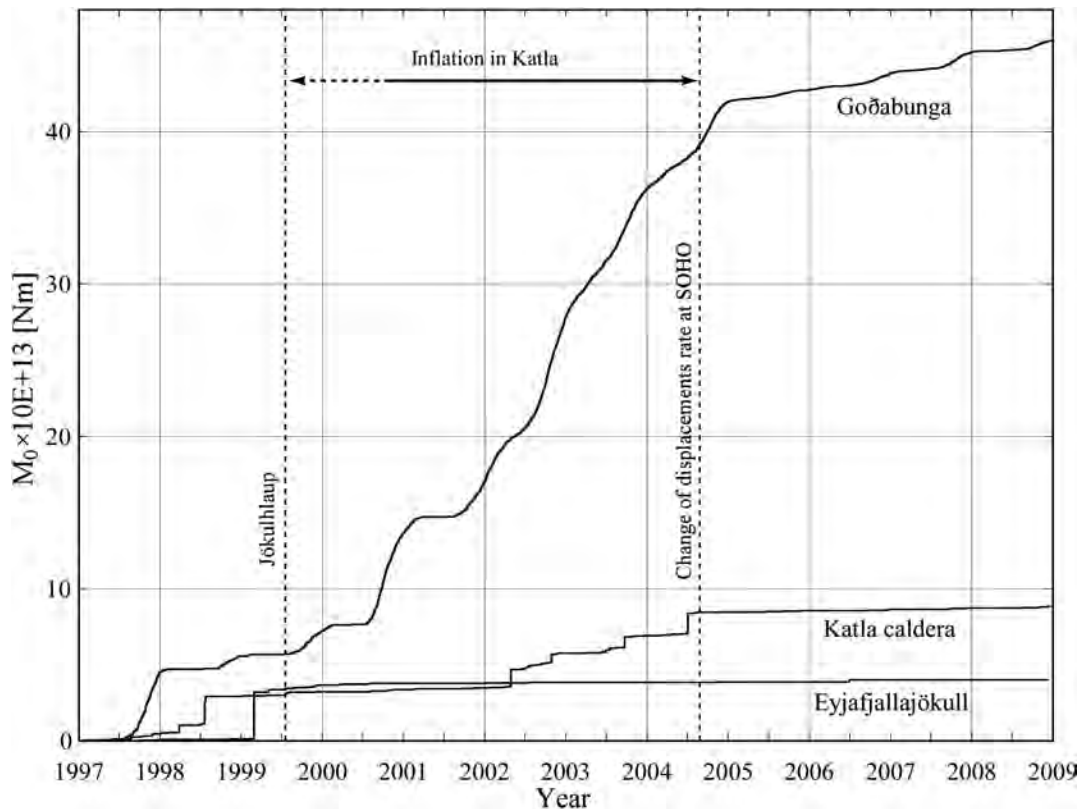
Fig. 2.4. Cumulative seismic moment released in the Katla caldera, the Goðabunga area and Eyjafjallajökull region, for the time period from 1 January, 1997, to 1 January, 2009. All earthquakes larger than magnitude $0.5M_{LW}$ are used in the moment-magnitude relation $\log M_0 = 1.5M_{LW}+9.1$, where M_0 is the seismic moment (Nm) and M_{LW} the local moment magnitude. Of the three regions, Goðabunga is by far the most active with continuous activity. Between 2002 and the beginning of 2005, earthquakes took place year-round within the Goðabunga region. Note that a new ice cauldron (Sturkell et al., 2008) was formed before the onset of sustained earthquake activity in the Goðabunga region. The character of the seismicity within the Katla caldera and in the Eyjafjallajökull volcano is more swarm-like. The 1999 swarm in Eyjafjallajökull was accompanied by a shallow intrusion. The vertical line in July 1999 represents the jökulhlaup that drained from Mýrdalsjökull (emanating from the Sólhemajökull). The vertical line in late August 2004 represents the change of displacements rate at SOHO continuous GPS-station.

these groups are quite distinct and different from one another.

Seismicity at Eyjafjallajökull is episodic by nature (Fig. 2.8A). In fact, most of the time, Eyjafjallajökull is almost aseismic. Three episodes of seismicity occurred in the 1990s, in 1994, 1996 and 1999 (Jakobsdóttir, 2008; Dahm and Brandsdóttir, 1997). The 1994 and 1999 episodes were associated with intrusive activity beneath the SE flank of the volcano (Sturkell *et al.* 2003; Pedersen and Sigmundsson, 2004, 2006); the 1996 episode was much smaller and may have been related to the development of a conduit feeding the shallow intrusions (Fig. 2.8A). The beginning of each of the active periods seems to indicate that the semi-vertical conduit is located beneath the northern flank, whereas the magma was subsequently intruded southwards as sills at 4–6 km depth beneath the south-eastern flank. Most of the earthquakes at Eyjafjallajökull are high-frequency events of low magnitude but with sharp P- and S-waves. They have only once reached magnitude 3, preceding the beginning of the 1999 intrusion.

The Katla caldera epicentral cluster is not quite concentric with the caldera: its centre is displaced slightly

to the NE with respect to the caldera centre (Fig. 2.7). The largest magnitude earthquakes of the whole area take place within this cluster. The largest event recorded so far was that of June 2, 1977 (m_b 4.9; M_S 5.0, body-wave magnitude and surface-wave magnitude, respectively). There is still some controversy regarding the depth of the caldera earthquakes. Arrival time data for most of the events are consistent with a shallow source, 0–5 km, but deeper sources are not excluded (Vogfjörð and Slunga, 2008). The epicentral cluster is located in the same general area as the low-velocity, high-attenuation body detected by Guðmundsson *et al.* (1994) and interpreted as a magma chamber at a shallow level. It is therefore plausible that the earthquakes are related to stress changes around and above this chamber induced by pressure changes. The appearance of the earthquakes on the seismograms is consistent with this interpretation. They are mostly high-frequency events with some events that would probably classify as hybrid events. The focal mechanism studies that have been conducted on the Katla caldera events so far seem to indicate a large component of reverse faulting (Einarsson, 1987; Sturkell *et al.*, 2008). It is possible that some of the seismic activity is related to the extensive geothermal
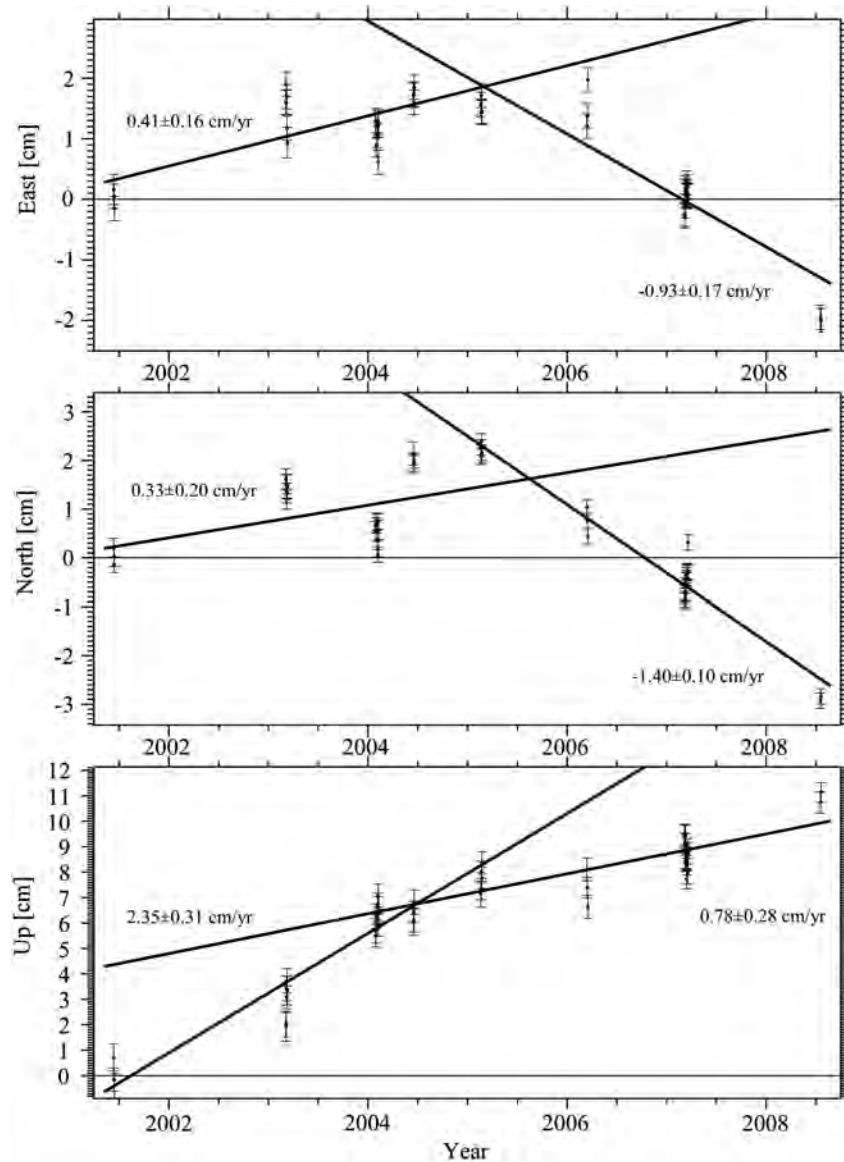
Fig. 2.5. Displacement time series for the campaign GPS site AUST from 2001 to 2008. Horizontal displacements are relative to stable Eurasia but the uplift relative to ITRF 2005 reference frame. The uncertainty is the square of covariance weighted from the least square fit. The sloping lines here, as well as in Fig. 2.11, represent the best line fit before and after August 2004. The displacement rate changed in late August 2004, and this is suggested to represent the termination of the inflation episode.

activity of the Katla caldera region as expressed by the many cauldrons in the ice surface, particularly along the caldera rims (Guðmundsson *et al.*, 2007). The geothermal water systems cool the crust as heat is mined from the magma chamber roof. The stress changes associated with the cooling and contracting crustal rocks may lead to earthquakes.

The Goðabunga earthquake cluster provides some of the most unusual aspects of the seismicity at Mýrdalsjökull. The earthquakes are almost exclusively of the low-frequency type, and this area is one of few areas in Iceland that consistently produce such earthquakes (Soosalu *et al.*, 2006a, 2006b). The earthquakes are often poorly recorded and typically have emergent P-waves, an unclear S-wave and a long low-frequency coda. This makes them difficult to locate. Furthermore, the magnitude scale for these earthquakes is problematic. Because of the long coda, they have a low amplitude/duration ratio, very different from that of 'normal' earthquakes. Magnitudes that are based on maximum amplitude are therefore likely to underestimate the size of the event. Another unusual aspect of the Goðabunga earthquakes is their pronounced seasonal correlation, first described by Tryggvason (1973). The correlation was later confirmed by Einarsson and Brandsdóttir (2000) who point out that both seasonal ice load change and resulting pore pressure change at the base of the ice could induce the modulation of the earthquakes. They argue that the pore pressure effect may be greater than the load effect, which is also consistent with the phase lag of the earthquakes with respect to the time of maximum deloading. The peak in the earthquake activity usually occurs during the fall months, 2–3 months after the maximum in the rate of deloading (Jónsdóttir *et al.*, 2007).
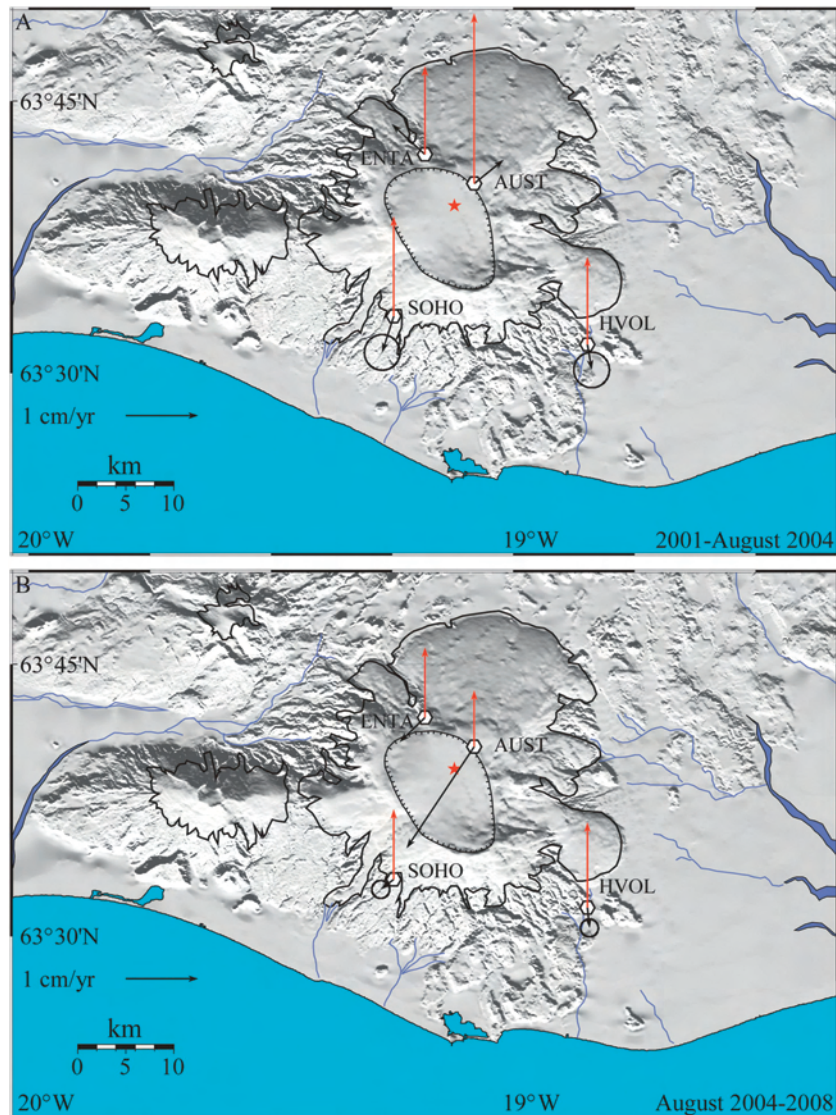
Fig. 2.6. (A) Observed horizontal and vertical displacements at Katla from 2001 to late August 2004, measured by GPS. Black arrows show horizontal displacement, and red arrows show vertical movements. Horizontal displacements are relative to stable Eurasia and vertical displacements are relative to the ITRF2005 reference frame. This uplift and outward displacement from a centre inside the Katla caldera (marked by a red star) suggests magma inflow in a magma chamber, which is possibly located at 3–5 km depth. (B) Observed horizontal and vertical displacements at Katla from the termination of the magmatic uplift in late August 2004 until end of 2008, measured by GPS. Black arrows show horizontal displacement, and red arrows show vertical movements. Horizontal displacements are relative to stable Eurasia and vertical displacements are relative to the ITRF2005 reference frame.

It has been suggested that the Goðabunga cluster is an expression of a rising cryptodome (Einarsson *et al.*, 2005; Soosalu *et al.*, 2006a), that is, a diapir-like volume of viscous magma beneath the surface. Several lines of arguments support this interpretation:

1. The low-frequency characteristics of the earthquakes are typical for dome activity.
2. The deformation field around Goðabunga is very localized. No deformation is detected at nearby tilt and GPS stations. This is one of the characteristics of rising domes (e.g. Poland and Lu, 2008).
3. The earthquake activity is remarkably persistent. There are fluctuations on a months-to-years time scale, but the day-by-day activity is steady.

4. The earthquake cluster is very tight and localized.
5. Geographical position of the cluster with respect to the Katla caldera is the same as for a number of acidic extrusive bodies. They appear to form an aureole around the caldera. Similar relationship is observed at some other central volcanoes in Iceland, such as Krafla (Jónasson, 1994).

Arguments have also been presented for icequakes as the source of the Goðabunga activity (Jónsdóttir *et al.*, 2008). Icequakes are known from several places in the glaciated areas of Iceland, in particular, along the edges of active glaciers and along the largest ice stream of Iceland, the Skeiðarárjökull tongue of Vatnajökull (e.g. Brandsdóttir and Menke, 1990; Roberts *et al.*, 2006).
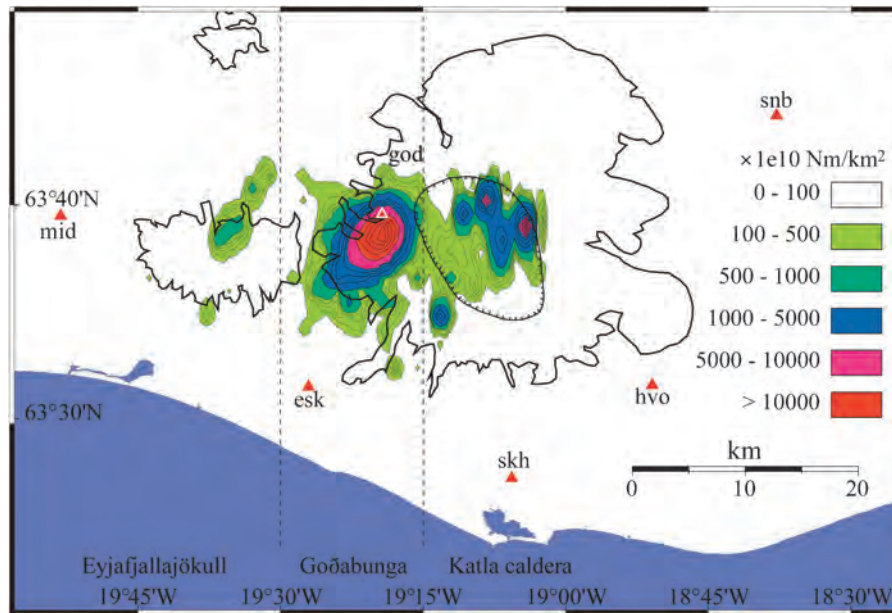
Fig. 2.7. Earthquake activity recorded from 1 January, 1997, to 1 January, 2008, in Eyjafjallajökull and Katla. Contours depict the cumulative seismic moment per square kilometre for the period. Seismic moment was calculated using the moment-magnitude relation $logM_0 = 1.5M_{LW}+9.1$. Earthquake activity is focused in three regions, separated by dashed lines: two in the Katla volcano; the area within the Katla caldera (2,176 events) and the Goðabunga region (11,951 events), separated by the dashed line, and in Eyjafjallajökull (396 events). Triangles mark locations of seismic stations of the national network, called with the acronym SIL.

These events are, however, considerably smaller than the events at Goðabunga. Furthermore, it is difficult to see why icequakes would be concentrated in a tight cluster and be more intensive at Goðabunga than at other glacier edges in Iceland.

Although the seismicity of the Katla area is generally high and persistent, it is by no means constant. Episodes of enhanced activity are separated by longer periods of less intense seismicity. Notable were the two episodes of greatly elevated seismicity in 1967 and 1976–1977 and an episode of unrest that began in 1999 with a flash flood from Sólheimajökull (Fig. 2.3) (Sturkell *et al*., 2008). Even these episodes are different from each other and probably reflect different processes in the evolution of Katla volcano. The relative importance of the two clusters was comparable during the 1976–1977 episode (Einarsson and Brandsdóttir, 2000), whereas it has changed considerably throughout the 1999–2004 episode (Fig. 2.4). The relative importance of the Goðabunga cluster increased during the episode, and the Katla caldera activity decreased. Also, the seasonal correlation at Goðabunga has changed noticeably. The correlation was strong in 1995–2001, with almost total seismic quiescence during the early part of the year (Fig. 2.4). Then, the activity increased and extended into the quiet periods until the activity became continuous throughout the year. Seasonal correlation was still discernible, but the level of activity was higher than before. Then, in 2004, the activity subsided to the previous level. The maximum magnitudes appear to have diminished, but the quiet periods have not returned (see Fig. 4D of Jakobsdóttir, 2008). At the time of writing (March 2009), the activity level was only moderate, the seasonal correlation was visible, but the activity had continued through the year.

Historical eruptions of Katla have often been preceded by felt and sometimes even damaging earthquakes (e.g. Thoroddsen, 1925; Björnsson and Einarsson, 1981). The precursor time is of the order of half an hour to two hours. Comparing these events to the present activity at Katla, it is quite clear that the historical earthquakes must be either considerably larger than the events that have occurred lately or originate in a different part of the volcano. They demonstrate that a change in the seismicity pattern is to be expected before the outbreak of the next eruption of Katla.

2.7. Crustal Deformation

2.7.1. Tilt

In 1967, three levelling lines, 500–600 m in length (HOFD, KOTL and JOKV in Fig. 2.3), were installed to determine changes in tilt (so-called dry tilt) caused by pressure changes in the Katla volcano. The inflation in 1999–2004 is suggested to be caused by a pressure increase of a source at 4–5 km depth with its apex in the northern region of the caldera (Figs. 2.3 and 2.6A). These stations are located at least 10 km from the Katla caldera rim and even further away from the centre of inflation 1999–2005 and are insensitive to inflation rates of 2 cm/yr during the 1999–2005 pressure build-up in Katla. The uncertainty in tilt obtained from levelling lines is 2–3 μrad. To generate tilt of 2 μrad at the nearest station by pressure increase at 5 km depth, an uplift of about 40 cm is required. The nearest station is KOTL (Fig. 2.3) at 15 km distance from the centre of inflation in 1999–2005. The three tilt stations (KOTL, HOFD and JOKV,
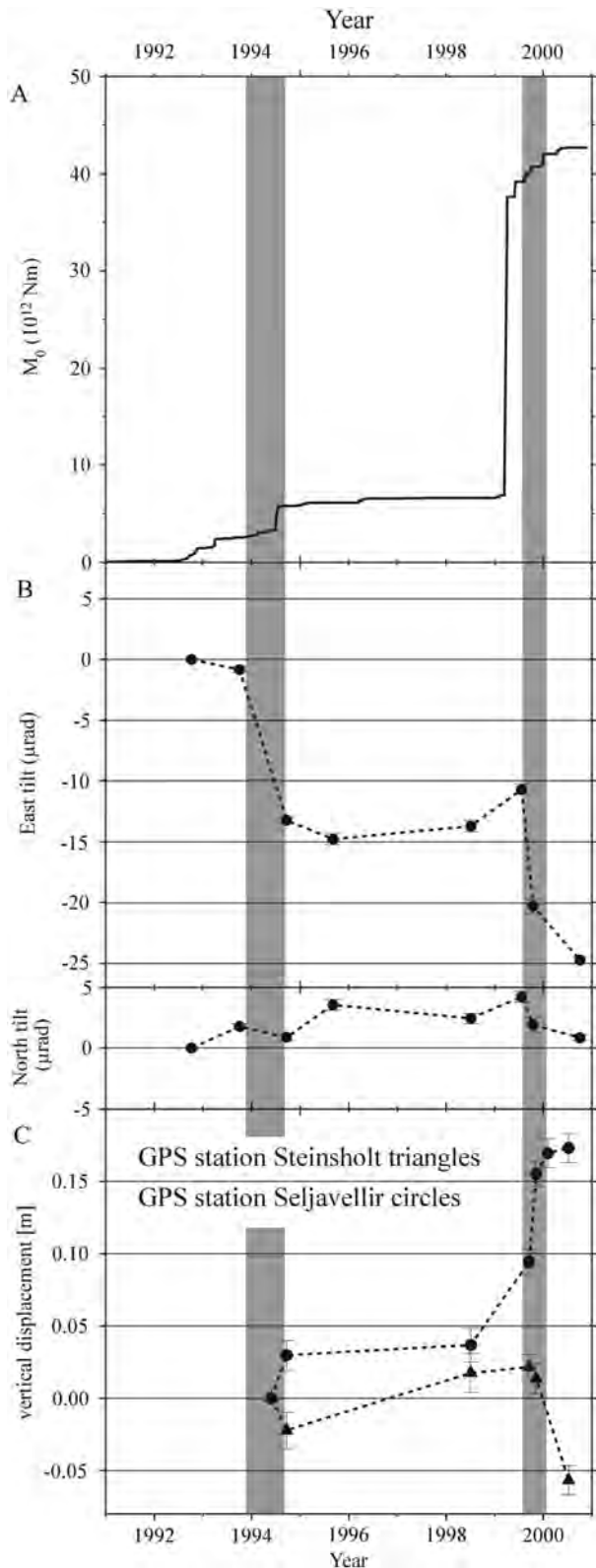
Fig. 2.3) are located too far away to be useful in detecting the current pressure changes in the inferred shallow magma camber in Katla.

A completely different story applies for the two tilt stations at each side of Eyjafjallajökull (Fig. 2.3), as they showed two inflation events (Fig. 2.8B). The crustal deformation caused by the two intrusion events (1994 and 1999) in Eyjafjallajökull gave distinct tilt signals at the two stations (DAGM and FIMM) flanking the volcano (Fig. 2.3). The station FIMM gave a clear signal of upward tilt pointing in the direction of the uplift (Figs. 2.8B and 2.9). The large tilt signal observed help to bracket the duration of the intrusions. The DAGM station was installed in 1994 after the first intrusion event. This station gave a clear signal, which was caused by the 1999 intrusion event and narrowed down the area of maximum uplift (Fig. 2.9), which was about half in size compared with the signal at FIMM.

The tilt station FIMM is favourably located for the detection of the deformation bulge on the south flank of Eyjafjallajökull, due to both the small distance and the size of the bulge (35 cm in 1999). A potential shallow deformation source at Goðabunga, on the contrary, does not produce a detectable signal at FIMM in spite of smaller distance. If the source at Goðabunga is located at 1.5 km depth, as the precise depth determinations of earthquakes seem to indicate (Soosalu *et al.* 2006a), the deformation field diminishes rapidly with distance, and the uplift must be of the order of 1 m to give a tilt of 2 μrad at FIMM. This indicates that the FIMM station will not be useful with only minor deformation at Goðabunga. However, the continuous GPS (CGPS) at GOLA (Fig. 2.3) is very sensitive to the localized deformation.

2.7.2. GPS

2.7.2.1. GPS processing

All data since 2000 have been processed with the Bernese software, version 5.0, using double-difference-based analysis with quasi-ionosphere-free (QIF) resolution strategy (Dach *et al.*, 2007). The final network solution is a minimum constraint solution, realized by three no-net-translation conditions imposed on a set of reference

Fig. 2.8. (A) Cumulative seismic moment of earthquakes in the Eyjafjallajökull volcano (from 1 January, 1991, to 1 January, 2002). Seismic activity intensified in the beginning of 1999, and this swarm continued into 2000. Thereafter, the earthquake activity has settled at a higher background level. The 1994 and 1999 periods of crustal deformation (intrusions) are shown as shaded bars (modified after Sturkell et al., 2003). (B) Observed ground tilt (1992–2002) at the optical levelling (dry) tilt station at Fimmvörduháls (installed in 1992), located between Mýrdalsjökull and Eyjafjallajökull (FIMM in Fig. 2.3). The strongest tilt signals are in an eastward direction in 1999. GPS data show that the tilt is a result of uplift under the southern slope of Eyjafjallajökull. (C) Time series of the vertical displacements at SELJ (Seljavellir) and STEI (Steinsholt) GPS stations (see Fig. 2.9) during the 1999–2000 intrusion event, the later subsidence of STEI probably is related to the closeness to the feeder channel. The tilt and GPS-measurements show clearly when the time periods of crustal deformation begin and end. They are shown as shaded bars. The 1999 crustal movement episode is well-constrained by deformation measurements and lags the seismic activity (modified after Sturkell et al., 2003).
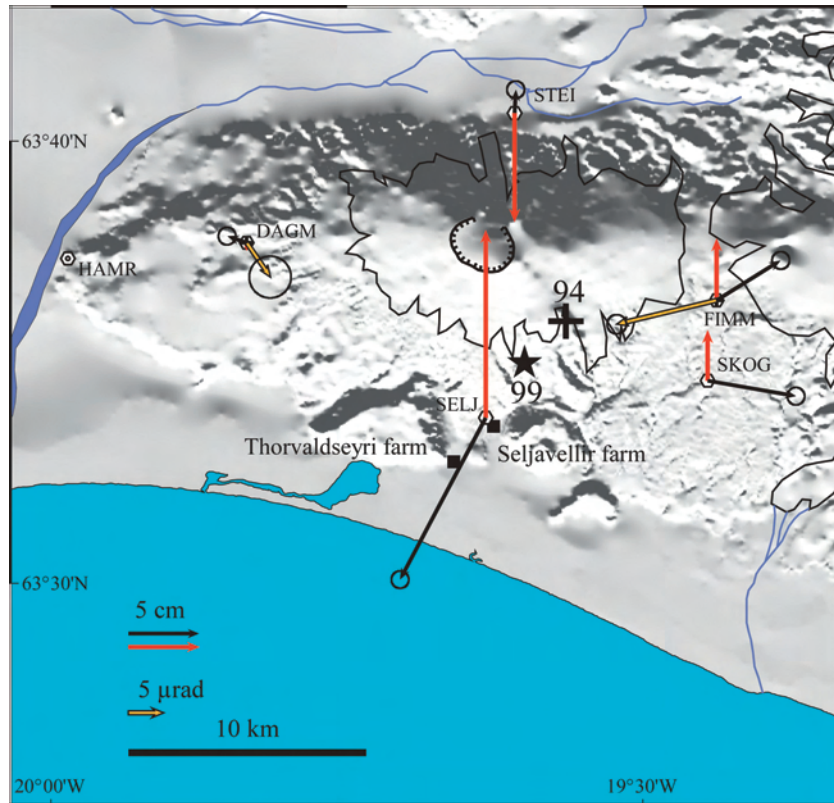
Fig. 2.9. *Observed horizontal and vertical displacements, relative to the GPS point HAMR, during the period from July 1998 to July 2000 for the GPS and tilt network around Eyjafjallajökull. Black arrows show horizontal displacement, and red arrows show vertical movements. Shaded arrows from station FIMM and DAGM show the tilt. The black star denotes a best-fit point source location for the 1999 episode, based on horizontal displacements. The suggested centre of uplift of the 1994 event is indicated with a plus sign. Black boxes indicate the location of the Thorvaldseyri and Seljavellir farms (modified after Sturkell et al., 2003).*

coordinates of GPS stations derived by the International GNSS Service (IGS). The set of IGS stations used includes stations in North America, Iceland and Scandinavia (REYK, HOFN, ALGO, ALRT, ONSA, TROM, MADR and WES2). The reference coordinates that are used are termed IGS05 and are a realization of the ITRF2005 reference frame (Altamimi *et al.*, 2007). The GPS-derived velocity field has then been plotted relative to stable Eurasia using the ITRF2005 absolute rotation pole for Eurasia (lat, lon, omega) = (56.330 deg, –95.979 deg, 0.261 deg/Myr) (Altamimi *et al.*, 2007). The same procedure is applied for both campaign and CGPS.

2.7.2.2. Campaign GPS

The campaign GPS network, which was directly aimed to follow the crustal deformation of the Katla volcano, was initiated in 1992. The GPS net was expanded in steps and today comprises about 25 stations (Fig. 2.3). Crustal deformation in the Katla region started in the neighbouring volcano Eyjafjallajökull in 1994. This led to the extension of the Katla GPS net to cover that volcano as well. As the GPS network around Eyjafjallajökull was in place, the intrusion stopped. However, the next intrusion in Eyjafjallajökull in 1999 had a good coverage of GPS sites, and the net was extended further.

All various GPS campaigns in the Katla and Eyjafjallajökull area, from 1992 to mid-2000, are listed in Sturkell *et al.* (2003). As the intrusive activity under Eyjafjallajökull ceased in the beginning of year 2000, inflation of the shallow magma chamber in Katla continued until the autumn of 2004. This transferred the focus of the campaigns to Katla. Since the termination of the inflation and reduction in earthquake activity in 2005, the GPS measurements at the Katla volcano have been limited to the sites installed on the two nunataks in Mýrdalsjökull (AUST and ENTA in Figs. 2.3 and 2.5). The complete network was measured in one survey for the first time in July 2000. Also, points in the Icelandic Land Survey network (ISNET) were included to provide ties to this network. The efforts concentrated on semi-annual surveys of the sites on the nunataks, as they were located close to the centre of uplift. The deformation rates turned out to be moderate and the deformation field did not reach far outside the Mýrdalsjökull ice cap. The two CGPS stations (SOHO and HVOL) together with the two campaigns sites boxed the deformation centre in Katla (Fig. 2.6A). With the geometry of the net and closeness to the inflation, the inferred location of the shallow magma chamber could be modelled (Fig. 2.6A).

From 2001 until 2003, constant uplift at AUST occurred at a rate of 1.7 cm/yr (Fig. 2.5), and radial displacement from the caldera centre was observed
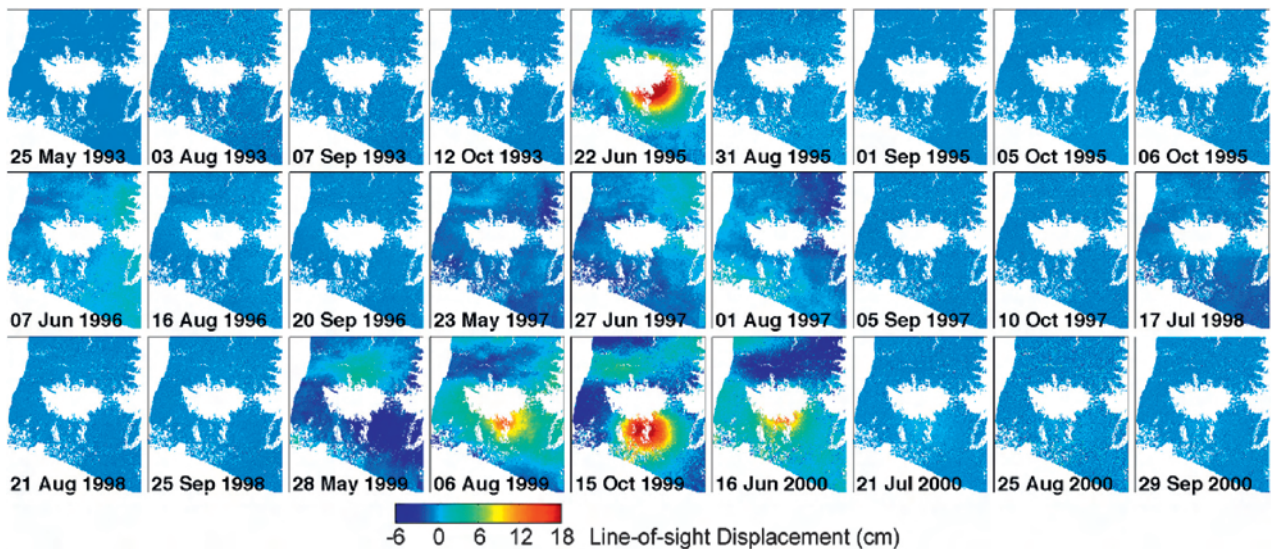
Fig. 2.10. Time series of the deformation field for Eyjafjallajökull volcano 1993–2000 based on InSAR data. The maps show the change in the line-of-sight to the radar satellites. The white area in the centre of each image corresponds to the outline of Eyjafjallajökull ice cap. Each image represents the incremental displacement since the time of the previous image, with reference to pixels in the northwest corner. Spatially correlated nuisance terms have been estimated and removed by spatial and temporal filtering (following Hooper et al., 2007), except for the 1999 images, where the temporal sampling is not high enough with respect to the deformation rate.

(Fig. 2.6A). Figure 2.6A shows the derived displacement vectors from benchmarks on and around Mýrdalsjökull in the Eurasia reference frame. A Mogi-point pressure model was used to calculate the best-fitting location of a point source. In the forward modelling, the horizontal displacements were given the largest weight, as those are much less sensitive to the glacio-isostatic readjustments, compared to the vertical component. GPS points on nunataks near the Katla caldera rim were displaced upwards and horizontally away from the centre at a rate of 1–2 cm/yr. The modelling gave a best-fitting point source at a depth of 4.9 km with an uplift amount of 12 cm at the centre of uplift.

In an attempt to monitor crustal deformation in the zone of maximum earthquake activity in the Goðabunga region (Fig. 2.3), the GPS benchmark (GOLA) was installed in 2004 to the immediate west of the ice cap. Within a six-month interval, 2.0 cm of uplift was detected at GOLA. From the summer 2006, a CGPS station occupies the same benchmark as the campaign measurements used.

Currently, campaign GPS is carried out once or twice per year, in March and if possible in June. The reason for performing the measurements at these times is logistical, as travelling on the glacier is easy during the spring and early summer. With the large annual variation in snow load, which gives a peak-to-peak amplitude of up to 1.2 cm, it is preferable to try to do the measurements during the same time each year to minimize the effect.

The campaign GPS measurements around the intrusion 1999–2000 in Eyjafjallajökull presented here use the Hamragarðar (HAMR, Fig. 2.3) benchmark as fixed in the processing. For a description of the processing procedure, see Sturkell *et al*. (2003). The displacement vectors for an intrusive event point outward from an area

on the south slopes of Eyjafjallajökull, indicating inflation (Fig. 2.9). The best-fitting Mogi source gave an estimate for the displacement of the reference station HAMR, resulting in the vector pattern. The 'best-fitting' Mogi model gives a displacement vector of 1.1 cm at 282° for the reference station. A maximum amount of vertical displacement, 35 cm, directly over the point source at a depth at 3.5 km, was inferred by modelling. The star denotes the best fit for the point source location in the 1999 episode by using the GPS and tilt data (Fig. 2.9). The InSAR data gave a much better model of the geometry of the intruding body (Fig. 2.10).

2.7.2.3. Continuous GPS

Crustal deformation is currently recorded at four CGPS sites around Mýrdalsjökull and Eyjafjallajökull (Fig. 2.3), to monitor volcanic deformation, co-seismic displacements and glacio-isostatic deformation (Geirsson *et al*., 2006). At the end of 2008, over 60 CGPS stations were in operation in Iceland, and most of them are deployed in the plate boundary deformation zone (Arnadottir *et al*., 2008). The CGPS data are automatically downloaded and processed on a daily basis with the result available on the Icelandic Meteorological Office website for public viewing (http://www.vedur.is). The time series from the CGPS stations are mostly dominated by plate spreading, but deviations are observed at stations close to individual volcanoes (Geirsson *et al*., 2006). The CGPS stations give excellent time resolution of volcanic activity, but due to high installation and operating costs, their spatial coverage is necessarily much sparser than that provided by campaign GPS.

In response to the unrest in Katla, two CGPS were installed, one at Sólheimaheiði (SOHO) and a second

at Láguhvolar (HVOL), south and south-east of Mýrdals-jökull, respectively, in late 1999 (Fig. 2.3). As most deformation in the late 1999 occurred in Eyjafjallajökull, the station Thorvaldseyri (THEY) was set up (Fig. 2.3). The benchmark of the CGPS station at THEY was installed in February 2000 and measured in that campaign, while the continuous measurements started in May 2000. At the time when the CGPS station at THEY became operational in May 2000, crustal deformation due to the intrusion in Eyjafjallajökull had ceased. The long-time trend shows no significant deformation signal that can be related to magma movements in Eyjafjallajökull. The fourth CGPS station in the area was Goðaland (GOLA) installed in 2006 over an existing campaign benchmark (Fig. 2.3).

The time series of displacement at SOHO relative to stable Eurasia (Fig. 2.11) have been corrected for the annual variation caused by the snow load. The station SOHO (and to some extent HVOL) shows southward displacement in excess of the plate movement since 2000, which we attribute to a local source of inflation in the Katla volcano. Applying a point source model for the inflation gives an outward horizontal displacement nearly three times larger than the vertical signal at the SOHO station (see Table 1 in Sturkell *et al.*, 2008). The vertical signal is a combination of glacio-isostatic uplift and the pressure increase in an inferred magma chamber, with the vertical signal caused by the magma chamber only marginal. The same applies for the HVOL station even to a greater extent. The horizontal signal caused by the pressure increase in the modelled shallow magma chamber under the Katla caldera is about a half of what is recorded at SOHO. During the period until early autumn 2004, the north component of SOHO has a rate of 0.5 cm/yr (Fig. 2.11). As the pressure increase apparently ceased in the later part of 2004, the rate of the north-south component slowed down to 0.14 cm/yr. No obvious changes in the displacement rates of the east and vertical components can be observed (Fig. 2.11). The ratio between the vertical and horizontal rates since 2004 is 4.2 (0.97 cm/yr of uplift and 0.23 cm/yr of movement outward from the caldera). Following Pinel *et al.* (2007), this implies that the current deformation signal at SOHO is probably dominated by glacio-isostatic response to the rapid ice-sheet reduction, which takes place at Mýrdalsjökull. A decrease of the seismic activity correlates with the change of deformation rate of the horizontal component at SOHO (Figs. 2.3 and 2.11).

The vertical time series at SOHO shows a seasonal variation, with a peak-to-peak amplitude close to 1.2 cm. In a study by Grapenthin *et al.* (2006), a correlation between the seasonal variation and the annual snow load in Iceland could be established. The model, based on the available CGPS data in Iceland, predicted a peak-to-peak amplitude seasonal displacement of 1.1 cm, at SOHO, which is in fair agreement with our time series, which were calculated in a slightly different manner than in Grapenthin *et al.* (2006). The deformation rate of the outward displacement at SOHO decreased in 2004 at approximately the same time as the seismic intensity decreased (Figs. 2.4 and 2.11). We suggest this marks the termination of the inflation event in Katla volcano, which started in 1999.

2.7.3. *InSAR*

Spaceborne InSAR is a valuable tool for measuring surface deformation because of the high spatial resolution achieved and the ability to acquire the data remotely. Nevertheless, significant issues arise due to changes in scattering properties of the Earth's surface, variations in atmospheric path delay and inaccuracies in satellite orbit and surface elevation determination. Time series InSAR techniques provide a way to address the issues. Currently, there are two broad categories of these techniques, persistent scatterer methods (e.g. Ferretti *et al.*, 2001; Hooper *et al.*, 2004; Kampes, 2005) and small baseline methods (e.g. Berardino *et al.*, 2002; Schmidt and Bürgmann, 2003). Hooper (2008) developed a new algorithm that combines the two approaches to maximize the spatial coverage of useful signal and allow more reliable estimation of integer phase cycle ambiguities present in the data.

In Hooper *et al.* (2009), the new algorithm was applied to 27 images acquired over Eyjafjallajökull volcano by ERS-1 and ERS-2 satellites in a descending look direction between May 1993 and September 2000 (Fig. 2.10). Two intrusive episodes could be detected, the first of which occurred in 1994 and the second of which began in mid-1999 and ended in early 2000. The deformation caused by the two episodes is clearly centred at different locations, which was also the conclusion of Pedersen and Sigmundsson (2006) from conventional InSAR analysis. However, the overall inferred deformation pattern for each episode is more regular than deduced from conventional InSAR due to the removal of digital elevation model and atmospheric artefacts and more accurate phase unwrapping in the time series analysis. In addition, the displacements during the 1999 episode are decomposed into four sequential steps by the time series processing. The data for both episodes can be explained by an intrusion of a circular sill with a uniform overpressure. Seismicity is interpreted to be mostly associated with a narrow magma feeder channel from depth that does not cause noticeable deformation.

The 1999 increase in seismicity at Eyjafjallajökull was associated with significant inflation of the volcano. The deformation data are modelled using InSAR by Pedersen and Sigmundsson (2006), Hooper *et al.* (2007), Hooper (2008) and by GPS and tilt by Sturkell *et al.* (2003). The inflation was centred to the southern flank of the volcano approximately 4 km south of the summit crater. Maximum uplift of the model is about 0.35 m. The application of Synthetic Aperture Radar (SAR) interferometry greatly supplements other, sparse surface deformation measurements from the Eyjafjallajökull. At Eyjafjallajökull, two deformation events in 1994 and 1999 are consistent with the intrusion of approximately circular, horizontal sills. For the latter event, we are able to resolve the evolution of the deformation in time; it appears the growth history of the sill is not, however, simple. The two intrusion events were associated with elevated earthquake activity. The earthquakes are not spatially constrained to the centre of uplift on the southern slope but are also to a large extent located below the northern slope of Eyjafjallajökull. Almost all earthquakes in 1994 occurred in the north; this
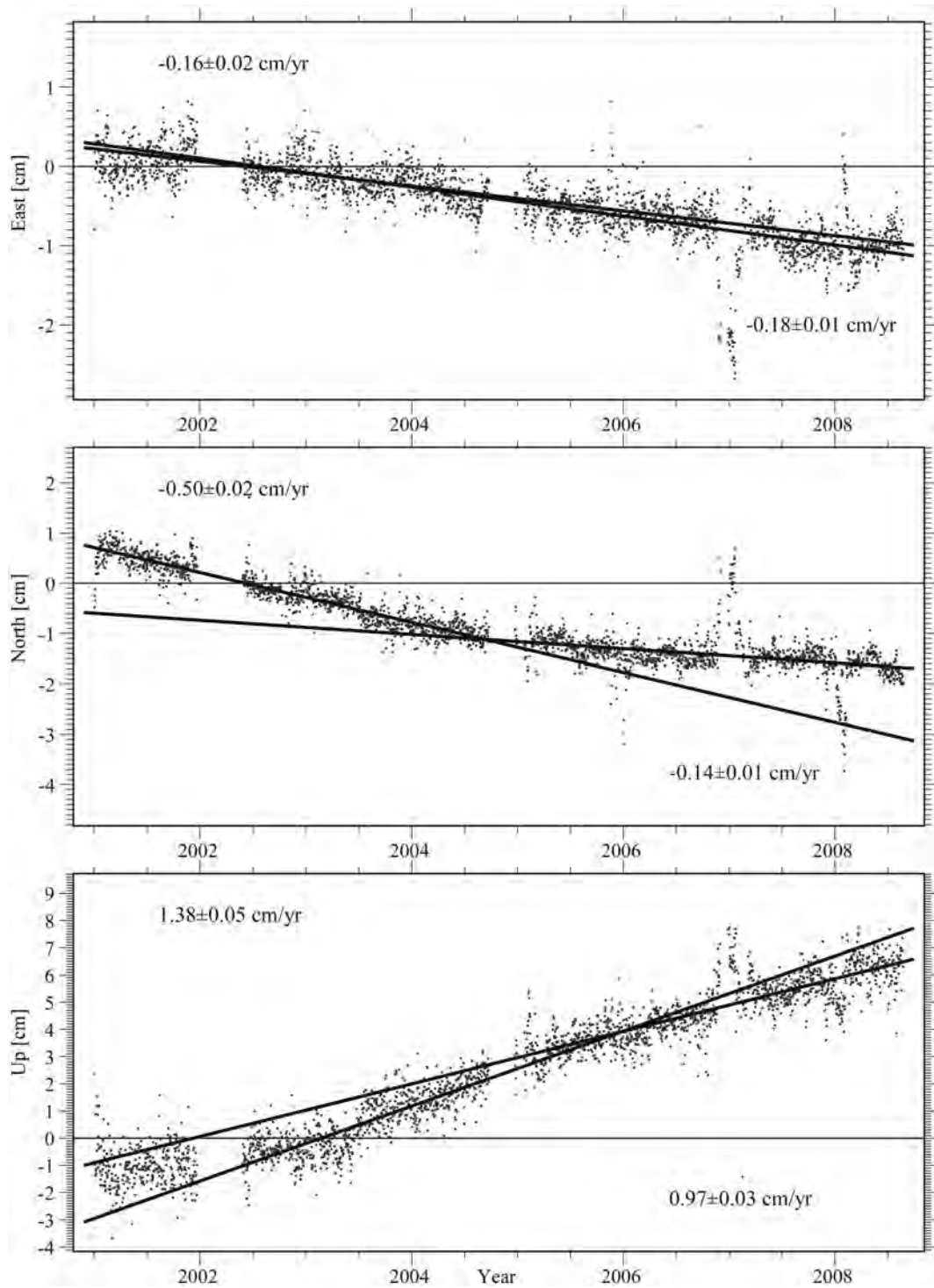
Fig. 2.11. Time series plot of displacement at SOHO. The horizontal displacements are relative to stable Eurasia but the uplift relative to ITRF 2005 reference frame. The uncertainty is the square of covariance from the weighted least square fit. The sloping lines indicate the displacement rates, and the most obvious change in rate appears in the north-south horizontal component. The rate changed in late August 2004, and this is suggested to represent the termination of the inflation episode. Annual variations in all components have been estimated and removed from the time series. In the vertical, we estimate a peak-to-peak amplitude of 1.2 cm. The time series of all three components shows that during a short time, an erratic behaviour of the calculated displacements takes place. This occurs in late 2006/early 2007 and in early 2008, and it is caused by accumulation of ice on different parts of the antenna.

pattern changed slightly in the 1999 episode, with some earthquakes occurring in the south. The majority of the earthquakes preceded the sill formation by half a year (Fig. 2.8A) and were spatially located in the northern part of Eyjafjallajökull (Fig. 2.7). This early cluster of earthquakes may be related to the feeder dike of the sill. Earthquake activity continued during the emplacement of the sill, which took about half a year.

Hooper *et al*. (2009) also applied the new time series InSAR algorithm to ERS and ENVISAT data acquired over Katla. No significant systematic motion was detected on the flanks of Katla from 1995 to 1998 and from 2000 to 2006, other than that expected from thinning of Vatnajökull and Mýrdalsjökull ice caps.

2.8. Discussion

Extensive crustal deformation research utilizing GPS geodesy and satellite radar interferometry provides constraints on magmatic unrest at the neighbouring subglacial volcanoes Katla and Eyjafjallajökull in 1994–2004. A decade long unrest period at these twin volcanoes began in 1994 with a sill intrusion under the Eyjafjallajökull volcano, followed by another sill intrusion in 1999. The onset of the second sill intrusion under Eyjafjallajökull occurred at a similar time as the 1999 jökulhlaup at Katla. Our measurements suggest that a modest inflow of magma towards shallow levels continued at Katla from 1999 until 2004. The active deformation sources are shown schematically in Fig. 2.12.

Crustal deformation measurements in the Mýrdalsjökull area have revealed movements that are caused by several processes. Interpretation of crustal deformation at subglacial volcanoes requires detailed consideration of the role of both load-induced deformation and deformation due to magmatic sources. Crustal deformation of the Mýrdalsjökull region appears to be affected by at least three common sources of deformation: (1) glacio-isostatic uplift due to thinning of the ice cap (Pinel *et al*., 2007,

2009), (2) an annual cycle in ground movements due to variable ice load (Grapenthin *et al*., 2006) and, in addition, (3) magmatic processes, as witnessed by the outward horizontal displacements from an area in the centre of the Katla caldera, as well as excessive uplift rate in 1999–2004. The time-dependent unrest in the Katla volcano is also manifested by elevated seismic activity. The dominant crustal deformation of the Katla volcano from the late 2004 and onwards can be attributed to rebound due to thinning of the Mýrdalsjökull ice cap. Ice thinning is well constrained for the period 1999–2004. Repeated radar altimeter measurements from an aircraft between 1999 and 2004 indicate a loss of over 3 km^3 of ice during that time, primarily from the margins of the ice cap (Pinel *et al*., 2007). Beneath and at the edge of an ice cap, vertical uplift dominates as the crustal response to ice loss, with horizontal displacements an order of magnitude less (ratio < 0.3) (Pinel *et al*., 2007, 2009); this applies to both the immediate elastic response and to the final, relaxed state of the crust. For a point source approximation of a magma chamber, the ratio between vertical displacement and horizontal is > 0.5. For Katla, Pinel *et al*. (2007) showed that the observed ratio nears 1. Furthermore, the rate of horizontal displacement is 1–2 cm/yr away from the Katla caldera edge, implying that observed horizontal deformation is principally due to magma accumulation. However, most of the vertical component of displacement observed outside the ice cap is likely due to glacio-isostatic response.

Seismicity at Goðabunga is remarkably regular, persistent and spatially concentrated (Fig. 2.7). Precise hypocentral locations reveal a zone of seismicity at 1.5 km depth (Soosalu *et al*., 2006a). The displacement field associated with the earthquakes appears to be very localized; it is not detected at a tilt station 8 km away, and apart from GOLA, none of the GPS benchmarks are affected. The seasonal trend in earthquake activity in the Goðabunga region has been interpreted by Einarsson and Brandsdóttir (2000) as a triggering effect due to increased groundwater pressure within the volcano during
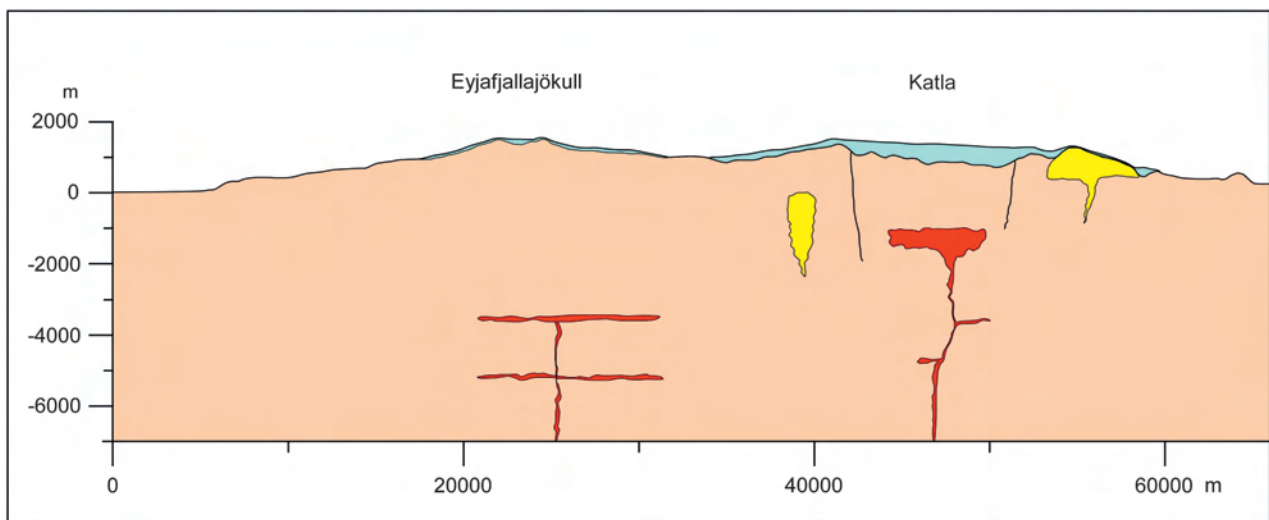

Fig. 2.12. Schematic cross-section from west to east across the Eyjafjallajökull and Katla volcanoes. Magmatic intrusions in 1994–2004 are drawn in red, rhyolitic domes and the cryptodome in yellow; glaciers are shown in light blue.

summertime melting of the overlying ice cap. More recently, Einarsson *et al.* (2005) and Soosalu *et al.* (2006a) have proposed that persistent earthquakes in the Goðabunga region are generated by an intruding cryptodome, that is, an ascending pocket of silicic or intermediate magma at shallow depth. This argument is based on the nature and style of the earthquake activity, the apparent displacement field, and the geographic proximity to the Katla caldera. Almost all outcrops of Katla rocks that are close to or immediately outside the caldera rim are silicic.

The inferred volume of magma accumulated in a shallow magma chamber at Katla during the 1999–2004 inflation period is approximately 0.01 km^3. This volume is miniscule compared to the erupted volume in 1918, when about 1 km^3 was erupted. The new magma was emplaced at shallow levels within the plumbing system of the Katla volcano. The high level of seismicity associated with inflation of the volcano during this period suggests that the volcano is close to failure and a new eruption or intrusion event may be initiated if magma flow towards shallow levels resumes. New material has been added to the shallow magma chamber, rather small volumes in this case, but this can thermally lubricate the pathways for deeper seated magma and give a fast track for the material to reach the surface. With the volcano in an agitated state, an eruption can take place without prolonged precursory signals. However, these effects decay with time as the magma solidifies unless new material is added.

Furthermore, the suspected cryptodome can cause explosive volcanism if it ascends above the ground and makes a dome, which can collapse and generate pyroclastic flows, or, if a basaltic magma intrudes into a rhyolitic cryptodome. In addition, basaltic eruptions that take place under the Mýrdalsjökull ice cap will be phreato-magmatic. This, together with a possible differentiation of the material in a shallow magma chamber, favours explosive activity, possibly reaching plinian magnitudes.

Acknowledgements

References

Altamimi, Z., Collilieux, X., Legrand, J., Garayt, B., & Boucher, C., 2007. ITRF2005: A new release of the International Terrestrial Reference Frame based on time series of station positions and Earth Orientation Parameters. Journal of Geophysical Research 112, B09401.

Arnadottir, T., Geirsson, H., Hreinsdottir, S., Jonsson, S., LaFemina, P., Bennett, R., Decriem, J., Holland, A., Metzger, S., Sturkell, E., & Villemin, T., 2008. Capturing crustal deformation signals with a new high-rate continuous GPS network in Iceland. Eos, Transactions, American Geophysical Union 89(53). Fall Meet. Suppl., Abstract G43A-0650.

Berardino, P., Fornaro, G., Lanari, R., & Sansosti, E., 2002. A new algorithm for surface deformation monitoring based on small baseline differential SAR interferograms. IEEE Transactions on Geoscience and Remote Sensing 40, 2375–2383.

Björnsson, S. & Einarsson, P., 1981. Jarðskjálftar - "Jörðin skalf og pipraði af ótta", Náttúra Íslands (2. útgáfa). Reykjavík, Almenna bókafélagið, 121–155.

Björnsson, H., Pálsson, F., & Gudmundsson, M.T., 2000. Surface and bedrock topography of Myrdalsjökull, South Iceland: The Katla caldera, eruption sites and routes of jökulhlaups.. Jökull 49, 29–46.

Brandsdóttir, B. & Menke, W., 1990. Icequakes in Entujökull and Kötlujökull. Jökull 39, 96–98.

Dach, R., Hugentobler, U., Frides, P., & Meindl, M., 2007. Bernese GPS software version 5.0. Switzerland, Astronomical Institute, University of Bern.

Dahm, T. & Brandsdóttir, B., 1997. Moment tensors of microearthquakes from the Eyjafjallajökull volcano in south Iceland. Geophysical Journal International 130, 183–192.

Eggertsson, S., 1919. Ymislegt smávegis vidvíkjandi Kötlugosinu 1918. Eimreidin 25, 212–222.

Einarsson, P., 1987. Compilation of earthquake fault plane solutions in the North Atlantic and Arctic Oceans. In: Kasahara, K. (Ed), Recent plate movements and deformation, Geodynamics Series, vol. 20, Washington, DC, American Geophysical Union, 47–62.

Einarsson, P., 1991. Earthquakes and present-day tectonism in Iceland. Tectonophysics 189, 261–279.

Einarsson, P. & Brandsdóttir, B., 2000. Earthquakes in the Myrdalsjökull area, Iceland, 1978–1985: Seasonal correlation and relation to volcanoes. Jökull 49, 59–73.

Einarsson, P. & Saemundsson, K., 1987. Earthquake epicenters 1982–1985 and volcanic systems in Iceland (map). In: Sigfússon, Th. (Ed), Í Hlutarsins Eðli: Festschrift for Thorbjorn Sigurgeirsson. Reykjavík, Menningarsjóður.

Einarsson, P., Soosalu, H., Sturkell, E., Sigmundsson, F., & Geirsson, H., 2005. Virkni í Kötlueldstödinni og nágrenni hennar sídan 1999 og hugsanleg thróun atburdarásar (Activity of Katla and surrounding area since 1999 and potential scenarios). In: Guðmundsson, M.T., Gylfason, Á.G. (Eds), Haettumat vegna eldgosa og hlaupa frá vestanverdum Mýrdalsjökli og Eyjafjallajökli (Assessment of hazard due to eruptions and jökulhlaups from western Mýrdalsjökull and Eyjafjallajökull). Reykjavík, Iceland, University Publ., 151–158.

Ferretti, A., Prati, C., & Rocca, F., 2001. Permanent scatterers in SAR interferometry. IEEE Transactions on Geoscience and Remote Sensing 39, 8–20.

Geirsson, H., Árnadóttir, Th., Völksen, C., Jiang, W., Sturkell, E., Villemin, T., Einarsson, P., Sigmundsson, F., & Stefánsson, R., 2006. Current plate movements across the Mid-Atlantic Ridge determined from 5 years of continuous GPS measurements in Iceland. Journal of Geophysical Research 111, B09407.

Grapenthin, R., Sigmundsson, F., Geirsson, H., Arnadottir, T., & Pinel, V., 2006. Icelandic rhythmics: Annual modulation of land elevation and plate spreading by snow load. Geophysical Research Letters 33, L24305.

Guðmundsson, M.T. & Högnadóttir, Þ., 2005. Ísbrádnun og upptakarennsli jöulhlaupa vegna eldgos í Eyjafjallajökull og vestanverdum Mýrdalsjökuli. (The melting distribution and origin of the jökulhlaups that can be caused by eruptions from western Mýrdalsjökull and Eyjafjallajökull). In: Guðmundsson, M.T., Gylfason, Á.G. (Eds), Haettumat vegna eldgosa og hlaupa frá vestanverdum Mýrdalsjökli og Eyjafjallajökli (Assessment of hazard due to eruptions and jökulhlaups from western Mýrdalsjökull and Eyjafjallajökull). Reykjavík, Iceland, University Publ., 158–179.

Guðmundsson, M.T., Högnadóttir, Þ., Kristinsson, A.B., & Guðbjörnsson, S., 2007. Geothermal activity in the subglacial Katla caldera, Iceland, 1999–2005, studied with radar altimetry. Annals of Glaciology 45, 66–72.

Guðmundsson, Ó., Brandsdóttir, B., Menke, W., & Sigvaldason, G.E., 1994. The crustal magma chamber of the Katla volcano in South Iceland revealed by 2-D seismic undershooting. Geophysical Journal International 119, 277–296.

Hooper, A., 2008. A multi-temporal InSAR method incorporating both persistent scatterer and small baseline approaches. Geophysical Research Letters 35, L16302.

Hooper, A., Pedersen, R., & Sigmundsson, F., 2009. Constraints on magma intrusion at Eyjafjallajökull and Katla volcanoes in Iceland, from time series SAR interferometry. In: Bean, C.J., Braiden, A.K., Lokmer, I., Martini, F., O'Brien, G.S. (Eds), VOLUME project, EU PF6 (No. 018471). ISBN 978-1-905254-39-2. VOLUME Project Consortium, Dublin.

Hooper, A., Segall, P., & Zebker, H., 2007. Persistent scatterer InSAR for crustal deformation analysis, with application to Volcán Alcedo, Galápagos. Journal of Geophysical Research 112, B07407.

Hooper, A., Zebker, H., Segall, P., & Kampes, B., 2004. A new method for measuring deformation on volcanoes and other natural terrains using InSAR persistent scatterers. Geophysical Research Letters 31, L23611.

Jakobsdóttir, S.S., 2008. Seismicity in Iceland: 1994–2007. Jökull 58, 75–100.

Jakobsson, S.P., 1979. Petrology of recent basalts of the eastern volcanic zone, Iceland. Acta Naturalia Islandica 26, 1–103.

Jóhannesson, H., Jakobsson, S.P., & Saemundsson, K., 1990. Geological map of Iceland, sheet 6, South-Iceland (third edition). Reykjavík, Icelandic Museum of Natural History and Geodetic Survey.

Jóhannsson, G., 1919. Kötlugosid 1918. (The Katla eruption of 1918). Reykjavík, Bókaverslun Ársaels Árnasonar, 72.

Jónasson, K., 1994. Rhyolite volcanism in the Krafla central volcano, North-East Iceland. Bulletin of Volcanology 56, 516–528.

Jónsdóttir, K., Tryggvason, A., Roberts, R., Lund, B., Soosalu, H., & Bödvarsson, R., 2007. Habits of a glacier covered volcano: seismicity and a structure study of the Katla volcano, South Iceland. Annals of Glaciology 45, 169–177.

Jónsdóttir, K., Roberts, R., Tryggvason, A., Lund, B., Pojhola, V., Jakobsdóttir, S.S., & Bödvarsson, R., 2008. Local lp-events study in a glaciated volcanic environment in south Iceland. Geophysical Research Abstracts 10, EGU2008-A-08854, EGU General Assembly, Vienna.

Jónsson, J., 1998. Eyjafjöll drög að jarðfraeði. Rannsóknstof-nunin Nedri Ás, Hveragerði, Ísland. Publ. 53, 1–111.

Jónsson, G. & Kristjánsson, L., 2000. Aeromagnetic measurements over Mýrdalsjökull and vicinity. Jökull 49, 47–58.

Kampes, B.M., 2005. Displacement parameter estimation using permanent scatterer interferometry. PhD Thesis. Delft University of Technology, Holland.

Lacasse, C., Sigurdsson, H., Carey, S.N., Jóhannesson, H., Thomas, L.E., & Rogers, N.W., 2007. Bimodal volcanism at the Katla subglacial caldera, Iceland: Insight into the geochemistry and petrogenesis of rhyolitic magmas. Bulletin of Volcanology 69, 373–399.

LaFemina, P.C., Dixon, T.H., Malservisi, R., Árnadóttir, T., Sturkell, E., Sigmundsson, F., & Einarsson, P., 2005. Geodetic GPS measurements in South Iceland: strain accumulation and partitioning in a propagating ridge system. Journal of Geophysical Research 110, B11405.

Larsen, G., 2000. Holocene eruptions within the Katla volcanic system, south Iceland: characteristics and environmental impact. Jökull 49, 1–28.

Larsen, G., Dugmore, A.J., & Newton, A.J., 1999. Geochemistry of historical-age silicic tephras in Iceland. The Holocene 9, 463–471.

Óladóttir, B.A., Larsen, G., Thordarson, Th., & Sigmarsson, O., 2005. The Katla volcano, S-Iceland: holocene tephra stratigraphy and eruption frequency. Jökull 55, 53–74.

Óladóttir, B.A., Sigmarsson, O., Larsen, G., & Thordarson, Th., 2008. Katla volcano, Iceland: Magma composition, dynamics and eruption frequency as depicted by the Holocene tephra layer record. Bulletin of Volcanology 70, 473–493.

Óskarsson, N., Sigvaldason, G.E., & Steinthórsson, S., 1982. A dynamic model of rift zone petrogenesis and the regional petrology of Iceland. Journal of Petrology 23, 28–74.

Pedersen, R. & Sigmundsson, F., 2004. InSAR based sill model links spatially offset areas of deformation and seismicity for the 1994 unrest episode at Eyjafjallajökull volcano, Iceland. Geophysical Research Letters 31, L14610.

Pedersen, R. & Sigmundsson, F., 2006. Temporal development of the 1999 intrusive episode in the Eyjafjallajökull volcano, Iceland, derived from InSAR images. Bulletin of Volcanology 68, 377–393.

Pinel, V., Sigmundsson, F., Sturkell, E., Geirsson, H., Einarsson, P., Guðmundsson, M.T., & Högnadóttir, T., 2007. Discriminating volcano deformation due to magma movements and variable surface loads: application to Katla subglacial volcano, Iceland. Geophysical Journal International 169, 325–338.

Pinel, V., Albino, F., Sigmundsson, F., Sturkell, E., Geirsson, H., Einarsson, P., & Guðmundsson, M.T., 2009. Consequences of local surface load variations for volcanoes monitoring: application to Katla subglacial volcano, Iceland. In: Bean, C.J., Braiden, A.K., Lokmer, I., Martini, F., O'Brien, G.S. (Eds), VOLUME project, EU PF6 (No. 018471). ISBN 978-1-905254-39-2. VOLUME Project Consortium, Dublin.

Poland, M.P. & Lu, Z., 2008. Radar interferometry observations of surface displacements during pre- and co-eruptive periods at Mount St. Helens, Washington, 1992–2005. In: Sherrod, D.R., Scott, W.E., Stauffer, P.H. (Eds), A volcano rekindled: the renewed eruption of Mount St. Helens, 2004–2006. Professional Paper 1750, United States Geological Survey, Menlo Park, CA, Chapter 18.

Rist, S., 1967. Jökulhlaups from the ice cover of Mýrdalsjökull on June 25, 1955 and January 20, 1956.. Jökull 17, 243–248.

Roberts, M.J., Magnússon, E., Bennett, R., Geirsson, H., Sturkell, E., Björnsson, H., Pálsson, F., & Rott, H., 2006. Meltwater dynamics beneath Skeiðararjökull from continuous GPS measurements and seismic observations. Eos, Transactions, American Geophysical Union 87(52). Fall Meet. Suppl., Abstract C31A-1232.

Schmidt, D.A. & Bürgmann, R., 2003. Time-dependent land uplift and subsidence in the Santa Clara valley, California, from a large interferometric synthetic aperture radar data set. Journal of Geophysical Research 108, 2416–2428.

Sigmundsson, F., 2006. Iceland geodynamics, crustal deformation and divergent plate tectonics. Chichester, Springer–Praxis Publishing Ltd, 209 pp.

Sigmundsson, F., Einarsson, P., Bilham, R., & Sturkell, E., 1995. Rift-transform kinematics in south Iceland: deformation from Global Positioning System measurements, 1986 to 1992. Journal of Geophysical Research 100, 6235–6248.

Sinton, J.M., Wilson, D.S., Christie, D.M., Hey, R.N., & Delaney, J.R., 1983. Petrological consequences of rift propagation on oceanic spreading ridges. Earth and Planetary Science Letters 62, 193–207.

Soosalu, H., Jónsdóttir, K., & Einarsson, P., 2006a. Seismicity crisis at the Katla volcano, Iceland – signs of a cryptodome? Journal of Volcanology and Geothermal Research 153, 177–186.

Soosalu, H., Lippitsch, R., & Einarsson, P., 2006b. Low-frequency earthquakes at the Torfajökull volcano, south Iceland. Journal of Volcanology and Geothermal Research 153, 187–199.

Sturkell, E., Einarsson, P., Roberts, M.J., Geirsson, H., Gudmundsson, M.T., Sigmundsson, F., Pinel, V., Guðmundsson, G.B., Ólafsson, H., & Stefánsson, R., 2008. Seismic and geodetic insights into magma accumulation at Katla subglacial volcano, Iceland: 1999 to 2005. Journal of Geophysical Research 113, B03212.

Sturkell, E., Einarsson, P., Sigmundsson, F., Geirsson, H., Ólafsson, H., Pedersen, R., De Zeeuwvan Dalfsen, E., Linde, A.T., Sacks, I.S., & Stefánsson, R., 2006. Volcano geodesy and magma dynamics in Iceland. Journal of Volcanology and Geothermal Research 150, 14–34.

Sturkell, E., Sigmundsson, F., & Einarsson, P., 2003. Recent unrest and magma movements at Eyjafjallajökull and Katla volcanoes, Iceland. Journal of Geophysical Research 108(B8), 2369.

Sveinsson, G., 1919. Kötlugosid 1918 og afleidingar thess (The Katla eruption of 1918 and its consequences). Reykjavík, Prentsmidja Gutenbergs, 61p.

Thórarinsson, S., 1975. Katla og annáll Kötlugosa. Árbók Ferdafélags Íslands. Ferdafélag Íslands, Reykjavík, 125–149.

Thordarson, T. & Larsen, G., 2007. Volcanism in Iceland in historical time: volcano types, eruption styles and eruptive history. Journal of Geodynamics 43, 118–152.

Thordarson, T., Miller, D.J., Larsen, G., Self, S., & Sigurdsson, H., 2001. New estimates of sulfur degassing and atmospheric mass-loading by the 934 AD Eldgjá; eruption, Iceland. Journal of Volcanology and Geothermal Research 108, 33–54.

Thoroddsen, Þ., 1925. Die Geschichte der isländischen Vulkane. Kongelige Danske Videnskabernes Selskab Skrifter, Naturvidenskabelig og Matematisk Afdeling, 8, Raekke, IX, Copenhagen, 458 pp.

Tryggvason, E., 1973. Seismicity, earthquake swarms and plate boundaries in the Iceland region. Bulletin of the Seismological Society of America 63, 1327–1348.

Vogfjörð, K. & Slunga, R., 2008. Imaging subsurface mass movement through relative earthquake locations in the Katla volcano, Iceland, and the possible location of a magma chamber. Reykjavík, Iceland, IAVCEI General Assembly.

Wessel, P. & Smith, W.H.F., 1998. New, improved version of generic mapping tools released. Eos, Transactions, American Geophysical Union 79(47), 579.